

J. Synchrotron Rad. (1999), **6**, 290–292

L_3 and $M_{4,5}$ absorption edges of intermediate valent cerium unravelled by resonant photoemission and resonant Auger spectroscopy

P. Le Fèvre^a, H. Magnan^{a,b}, J. Vogel^c, V. Formoso^d, K. Hricovini^{a,e} and D. Chandesris^a

^aLURE, Université Paris Sud, Bât. 209 d, BP 34, 91 898 Orsay Cedex (France)

^bCEA Saclay, DRECAM/SRSIM, 91 191 Gif sur Yvette (France)

^cLaboratoire Louis Néel, BP 166X, 38 042 Grenoble (France)

^dESRF, BP 220, 38 043 Grenoble Cedex (France)

^eLPMS, Université de Cergy-Pontoise (France)

In CeRh_3 and Ce_7Rh_3 compounds, strong resonant effects are observed in the Ce 3d and 4d photoemission spectra at the L_3 and $M_{4,5}$ absorption edges respectively. These resonances show unambiguously that interference effects exist in core level spectroscopies. In the CeRh_3 mixed valent compound, the resonances of photoemission peaks corresponding to $4f^0$, $4f^1$ and $4f^2$ final state character occur at different photon energies, making it possible to unravel the X-ray absorption profiles. Moreover, resonant $L_3M_{4,5}N_{4,5}$ Raman Auger lines are observed up to 10 eV above the L_3 absorption edge, showing the strong localized character of the core excited state.

Keywords: Resonant photoemission, resonant Auger, cerium, intermediate valent compounds

High energy resonant photoemission and resonant Auger spectroscopy are techniques which provide a direct information on the localization of electrons just above the Fermi level. In this paper, we present resonant 3d photoemission and resonant Auger measurements around the L_3 absorption edge and 4d photoemission around the $M_{4,5}$ absorption edges, both in trivalent and in mixed-valent Ce compounds (where Ce has an intermediate ground state, consisting in a mixing of trivalent ($4f^1(5d6s)^3$) and tetravalent ($4f^0(5d6s)^4$) electronic configurations).

XAS at the $L_{2,3}$ (Röhler, 1987) and $M_{4,5}$ (Kaindl, 1985) edges has been widely performed to study the electronic properties of rare earths (4f occupancy using phenomenological interpretation of the edge profiles (Röhler, 1987), or magnetism using X-ray Magnetic Circular Dichroism (XMCD) (Finazzi, 1995, Giorgetti, 1993, Kaindl, 1985)). Resonance experiments are a new way to assign the main structure of the absorption edge to precise final electronic configurations, for relatively localized states. Thus, fluorescence decay has allowed us to achieve a better understanding of the L_3 edge and the XMCD of rare earths (Krisch, 1995, Krisch, 1996, Bartolomé, 1997). The goal of the experiment is to give a clear explanation of the L_3 and $M_{4,5}$ edges profile, and a description of the transitions occurring in the absorption process.

The 3d photoemission lines of Ce were measured with photon energies around the Ce L_3 absorption edge (5723 eV). The experiment has been done at ESRF. The good energy resolution allowed us to isolate, in the CeRh_3 photoemission spectra, the satellites corresponding to mainly $4f^0$, $4f^1$ and $4f^2$

character of the final state (Figure 1(a)) (Fuggle, 1983). We have observed changes of about 25% in the relative intensities of the different 3d photoemission peaks when the excitative photon energy is varied across the L_3 edge. Along with observations on other La and Ce compounds (Vogel, 1995), these are one of the first observations of resonances for deep core levels. On the CeRh_3 mixed valent compound, we have performed CIS (Constant Initial State) measurements, i.e. the intensities of the different peaks of the photoemission spectrum as a function of the photon energy, across the Ce L_3 absorption edge. The results are presented on Figure 1(b). While the peak due to $4f^1$ final state resonates around 5728 eV (at the energy of the first structure of the Ce absorption edge), the $4f^0$ component resonates at 5738 eV (the position of the second structure of the Ce absorption edge). It is thus possible to assign unambiguously the two main lines in the XAS profile to $2p^54f^1$ and $2p^54f^0$ final states. The peak due to $4f^2$ final state resonates at a slightly lower photon energy than the $4f^1$ contribution, at the energy position of the shoulder due to $2p^54f^2$ states in the absorption spectrum (Bianconi, 1984). These experimental evidences confirm the phenomenological approach used to analyze the Ce XMCD signal by Giorgetti et al. (1993). The 3d photoemission spectrum of the Ce_7Rh_3 trivalent compound is presented on figure 1(a). It has a classical shape with mainly two $3d_{3/2}$ and $3d_{5/2}$ lines. These two lines resonates on the single white line of the L_3 absorption spectrum (see figure 2), at a photon energy of 5728 eV.

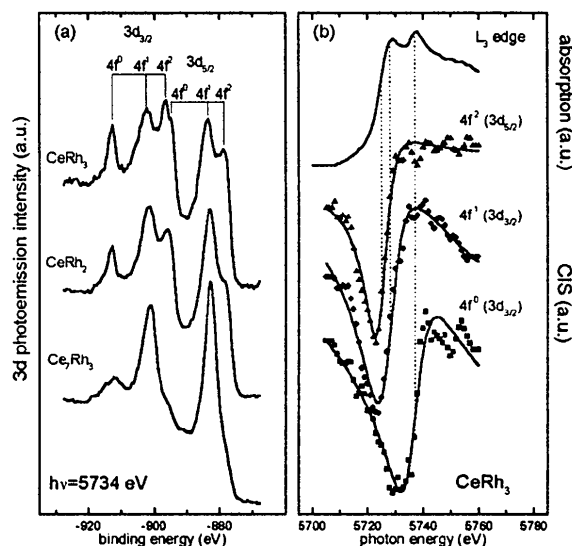


Figure 1

(a) Ce 3d photoemission spectra for different Ce-Rh compounds
(b) Different CIS spectra recorded on CeRh_3 , across the Ce L_3 absorption edge, for different contributions of the 3d photoemission spectra. Top part: the Ce L_3 absorption spectrum.

Resonant Auger measurements were performed on the same samples. The study was done on the $L_3M_{4,5}N_{4,5}$ Ce Auger lines, and the spectra, obtained at different photon energies across the Ce L_3 edge are presented on Figure 2. In the trivalent compound Ce_7Rh_3 , the spectra can be simply understood with the presence of a Raman-Auger process (double line appearing at constant binding energy), which resonates at the maximum of the white line of the XAS spectrum (5728 eV), and becomes afterwards the classical Auger process (at constant kinetic energy). The two main peaks of the Auger spectra can be attributed to the $L_3M_4N_{4,5}$ and $L_3M_5N_{4,5}$ lines.

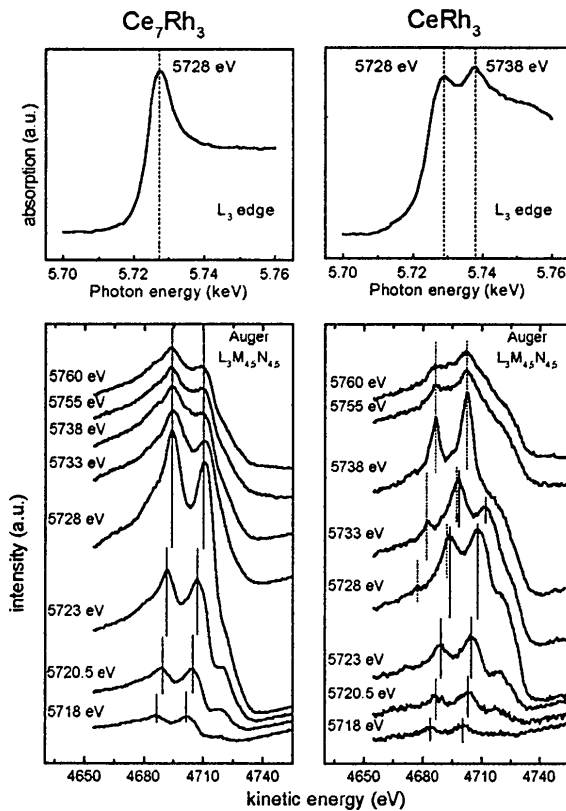


Figure 2

$L_{3,4,5}M_{4,5}N_{4,5}$ Auger spectra recorded on Ce_7Rh_3 (left part) and $CeRh_3$ (right part), at different photon energies across the Ce L_3 edge. Top part: the Ce L_3 absorption spectra for the two compounds.

In the $CeRh_3$ mixed valent compound, up to 5728 eV (and the maximum of the first structure of the XAS spectrum), we observe the Raman-Auger process at constant binding energy, with an increasing intensity. It consists of a double line at the same energy position than in the trivalent compound; it can therefore be attributed to a $4f^1$ Ce final state. A surprising fact is that this double line still disperses to higher kinetic energies for photon energies between 5728 and 5738 eV, which would indicate that the photoelectron created in this energy range (more than 10 eV above the edge) is still located on the absorbing atom. Between 5728 and 5738 eV, a second double line appears at varying kinetic energy, resonates at 5738 eV (at the maximum of the second structure of the XAS spectrum) and becomes afterwards the classical Auger process at constant kinetic energy. This second doublet, having a kinetic energy of 15 eV lower than the $4f^1$ doublet, can be attributed to a $4f^0$ configuration of Ce: the energy difference between the $4f^1$ and $4f^0$ Auger doublet is due to a better screening of the core holes by f as compared to valence electrons. At high energy, the $CeRh_3$ Auger spectra are dominated by the $4f^0$ final states. The relative intensities and positions of the classical Auger lines obtained in the two compounds have been very well reproduced by a fully atomic calculation (Hansen, 1998).

The resonances observed in the 3d photoemission peaks at the L_3 edge are caused by superposition of autoionization processes to the direct photoemission. In principle, resonances should be all the more intense as autoionization is probable, i.e. as the photoelectron is excited to a localized state. Therefore, resonances should be very strong at the $M_{4,5}$ absorption edges, where the photoelectron is excited to very localized 4f states. We have measured the Ce 4d photoemission lines in the same Ce_7Rh_3 and $CeRh_3$ compounds around the Ce $M_{4,5}$ absorption

edges. The experiments were done at LURE, on the SU23 beamline of the Super-ACO storage ring. The Ce $M_{4,5}$ absorption spectrum in the $CeRh_3$ intermediate valent compound is plotted in the top part of figure 3. For the Ce_7Rh_3 trivalent compound, the structures on the high energy side of the white lines disappear, and the absorption spectrum mainly shows two white lines. These structures are therefore attributed to $4f^0$ final states of the Ce atom. Like in the previous study of the L_3 edge profile, the resonant 4d photoemission study will provide an experimental evidence of this $4f^0$ origin.

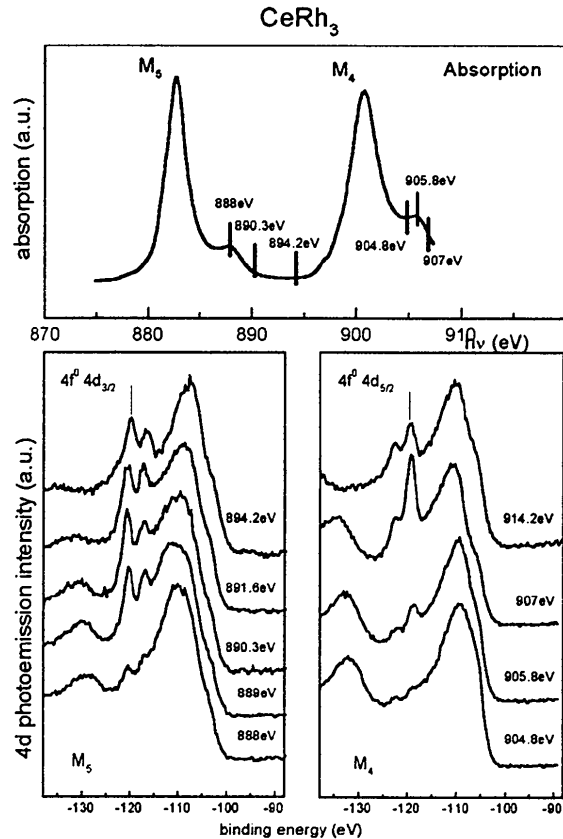


Figure 3

Ce $M_{4,5}$ absorption spectrum (top part), and different 4d photoemission spectra recorded for the indicated photon energies (bottom part), in the $CeRh_3$ compound.

For the $CeRh_3$ intermediate valent compound, some of the 4d photoemission spectra recorded with photon energies around the Ce $M_{4,5}$ absorption edges are presented in Figure 3. They consist of a large structure around 110 eV binding energy due to $4f^1$ and $4f^2$ characters of the Ce final state, and of two smaller structures around 120 eV binding energy, due to $4f^0$ character of the final state (labeled $4f^0(4d_{3/2})$ and $4f^0(4d_{5/2})$ in figure 3) (Fuggle, 1983). Figure 4 shows the CIS spectra for these different components in the photoemission spectra. It appears that the large $4f^1$ - $4f^2$ structure resonates strongly, slightly after the white lines of the M_5 and M_4 edges. During these resonances, the $4f^0$ satellites are drowned in the peak background, and their intensity can not be measured. The bottom part of figure 3 displays some of the photoemission spectra recorded while sweeping the photon energy across the high energy structure of the absorption thresholds: large changes in the relative intensities of the two $4f^0$ can be observed. The $4f^0(4d_{3/2})$ structure resonates mostly on the high energy side of the second bump of the M_5 edge ($3d_{5/2}$ levels); only a two times smaller resonance is measured on the second bump of the M_4 edge (see figure 4). A reverse behavior is

observed for the $4f^0(4d_{5/2})$: it resonates on the high energy side of the second bump of the M_4 edge ($3d_{3/2}$ levels), whereas almost no intensity change can be measured at the M_5 edge (see figure 4).

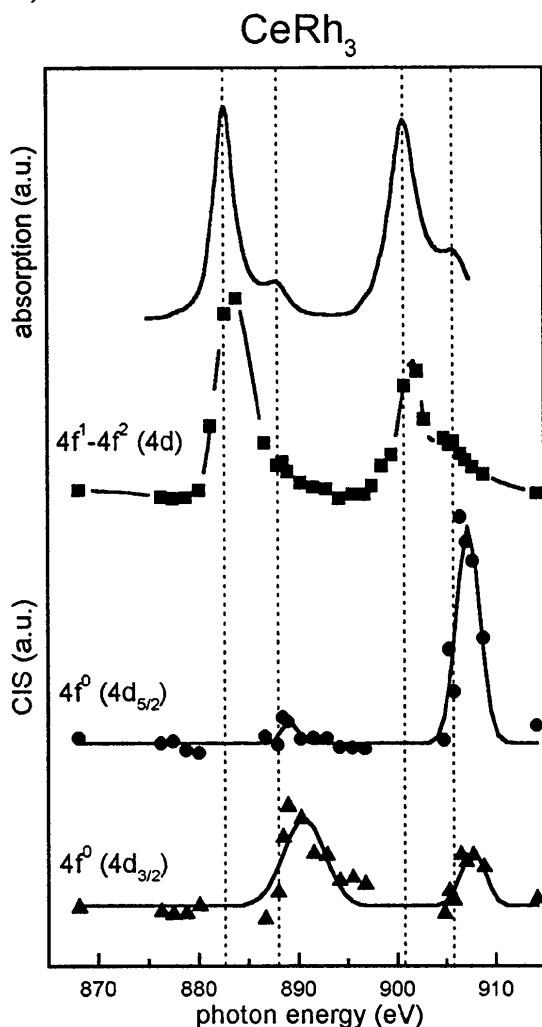


Figure 4

Ce $M_{4,5}$ absorption spectrum (top part), and CIS spectra recorded for the different lines of the Ce 4d photoemission (bottom part), in the $CeRh_3$ compound.

Like for the L_3 edge study, these resonance energies clearly evidence that the origin of the second structure of the $M_{4,5}$ edges are due to Ce $3d^9 4f^0$ final state. On the trivalent Ce_7Rh_3 compound, the 4d photoemission consists mainly of two close $4d_{3/2}$ and $4d_{5/2}$ peaks (Fuggle, 1983). The total structure formed by the two peaks resonates slightly after the maximum of the M_5 and M_4 white lines. The $4d_{3/2}$ peak resonates mainly on the high energy side of the M_5 ($3d_{5/2}$) edge, whereas the $4d_{5/2}$ peak resonates mainly on the high energy side of the M_4 ($3d_{3/2}$) edge.

As expected, we observed are very intense resonances at the $M_{4,5}$ edges. For these edges, a complete interpretation of the results can be done in a fully atomic formalism, the resonance effects being calculated in a coherent one step process (Nath, 1998).

References

Bartolomé, F., Tonnerre, J.M., Sève, L., Raoux, D., Chaboy, I.J., Garcia, L.M., Krisch, M. & Kao, C.C. (1997). *Phys. Rev. Lett.* **79**, 3775-3778.
 Bianconi, A., Marcelli, A., Davoli, I., Stizza, S. & Campagna, M. (1984). *Solid State Commun.* **49**, 409-415.

- Finazzi, M., de Groot, F.M.F., Dias, A.M., Kierren, B., Bertran, F., Sainctavit, Ph., Kappler, J.P., Schulte, O., Felsch, W. & Krill, G. (1995). *Phys. Rev. Lett.* **75**, 4654-4657.
 Fuggle, J. C., Hillebrecht, F. U., Zolnierok, Z., Lässer, R., Freiburg, Ch., Gunnarsson, O. & Schönhammer, K. (1983). *Phys. Rev. B* **27**, 7330-7341.
 Giorgetti, C., Pizzini, S., Dartyge, E., Fontaine, A., Baudalet, F., Brouder, C., Bauer, Ph., Krill, G., Miraglia, S., Fruchart, D. & Kappler, J.P. (1993). *Phys. Rev. B* **48**, 12732-12742.
 Hansen, J. (1998). Private communication.
 Kaindl, G., Kalkowski, G., Brewer, W.D., Sampathkumaran, E.V., Holtzberg, F., Schach, A. & Wittenau, V. (1985). *J. magn. magn. mater.* **47-48**, 181-189.
 Krisch, M. H., Kao, C.C., Sette, F., Caliebe, W.A., Hämäläinen, K. & Hastings, J.B. (1995). *Phys. Rev. Lett.* **74**, 4931-4934.
 Krisch, M. H., Sette, F., Bergmann, U., Masciovecchio, C., Verbeni, R., Goulon, J., Caliebe, W. & Kao, C.C. (1996). *Phys. Rev. B* **54**, R12673-R12676.
 Malterre, D. (1991). *Phys. Rev. B* **43**, 1391-1398.
 Nath, K. G., Ufuktepe, Y., Kimura, S., Kinoshita, T., Kumigashira, H., Takahashi, T., Matsumura, T., Suzuki, T., Ogasawara, H. & Kotani, A. (1998). *J. Electron Spectrosc. Relat. Phenom.* **88-91**, 369-375.
 Röhrer, J. (1987). "Handbook on Physics and Chemistry of Rare Earths", edited by K. A. Gschneider and J. Hüfner (North-Holland, Amsterdam), Vol. 10.
 Vogel, J., Magnan, H., Kappler, J.P., Krill, G. & Chandresris, D. (1995). *J. Electron Spectrosc. Relat. Phenom.* **76**, 735-740.

(Received 10 August 1998; accepted 9 December 1998)